Bridge Engineering

Residual life of historic riveted steel bridges: an analytical approach
Pipinato, Pellegrino and Modena

ice | proceedings

Proceedings of the Institution of Civil Engineers

http://dx.doi.org/10.1680/bren.11.00014
Paper 1100014
Received 24/03/2011 Accepted 15/09/2012
Keywords: bridges/steel structures/stress analysis

Residual life of historic riveted steel bridges: an analytical approach

1 **Dr Pipinato Alessio** Eng Arch
Research Associate, Department of Civil and Environmental Engineering, University of Padua, Padua, Italy

2 **Dr Pellegrino Carlo** Eng
Assistant Professor, Department of Civil and Environmental Engineering, University of Padua, Padua, Italy

3 **Modena Claudio** Prof, Eng
Full Professor, Department of Civil and Environmental Engineering, University of Padua, Padua, Italy


1


2


3

As a consequence of the increasing traffic demand, the life of a large stock of riveted bridges that still exist throughout the world must be extended, ensuring at the same time that safety is not compromised for economic reasons. As fatigue life estimation of metal historical bridges is a key issue for managing cost-effective decisions regarding rehabilitation or replacement of existing infrastructure, there is a need to estimate how long these structures could remain in service. In this paper, a fatigue assessment of a common short-span railway bridge is analysed and assessed. Based on analytical and parametric studies, the remaining life of the bridge is presented and discussed.

Notation

A_g	gross area of rivets
A_v	shear area of rivets
C	global damping matrix of the bridge
D_d	total damage index
d_d	annual damage index
K	global stiffness matrix of the bridge
L_ϕ	determinant length of the member (m)
M	global mass matrix of the bridge
N_t	endurance
n_o	approximate natural frequency (Hz)
n_t	number of cycles
P_t	set of axle load vectors at each discrete time
$P(t)$	axle load time history vector of trains
T_{RF}	remaining fatigue life of the detail
$U(t)$	displacement time history vector of the bridge at discrete times
$U(t_t)$	displacement vector of the bridge at discrete times
$\dot{U}(t)$	velocity time history vector of the bridge at discrete times
$\ddot{U}(t)$	displacement vector of the bridge at discrete times
v	commissioning speed of trains (m/s)
β	traffic volume parameter
δ_0	maximum mid-span deflection of the longitudinal girder under permanent loading (mm)
γ_{MF}	fatigue strength partial safety
$\Delta\zeta$	train–bridge inertial interaction, accounted by additional modal damping (%)
η	traffic speed parameter
φ''	dynamic amplification factor

1. Introduction

Fatigue failure is clearly a matter of on-going concern, particularly as fatigue damage is the factor that directly or indirectly accounted for the failure of most bridges in the past. The concern arises especially on railway lines which carry heavy traffic and for which further increases in the number and speed of trains are expected. Riveting technology was very popular from about 1860 to 1950 and most of the steel construction in that period was assembled by this technology. Rivets were often used in bridge building because they can provide a tight fitting connection. After welding and bolting were introduced and developed (about 1950), the use of rivets declined. However, there are still many riveted structures in

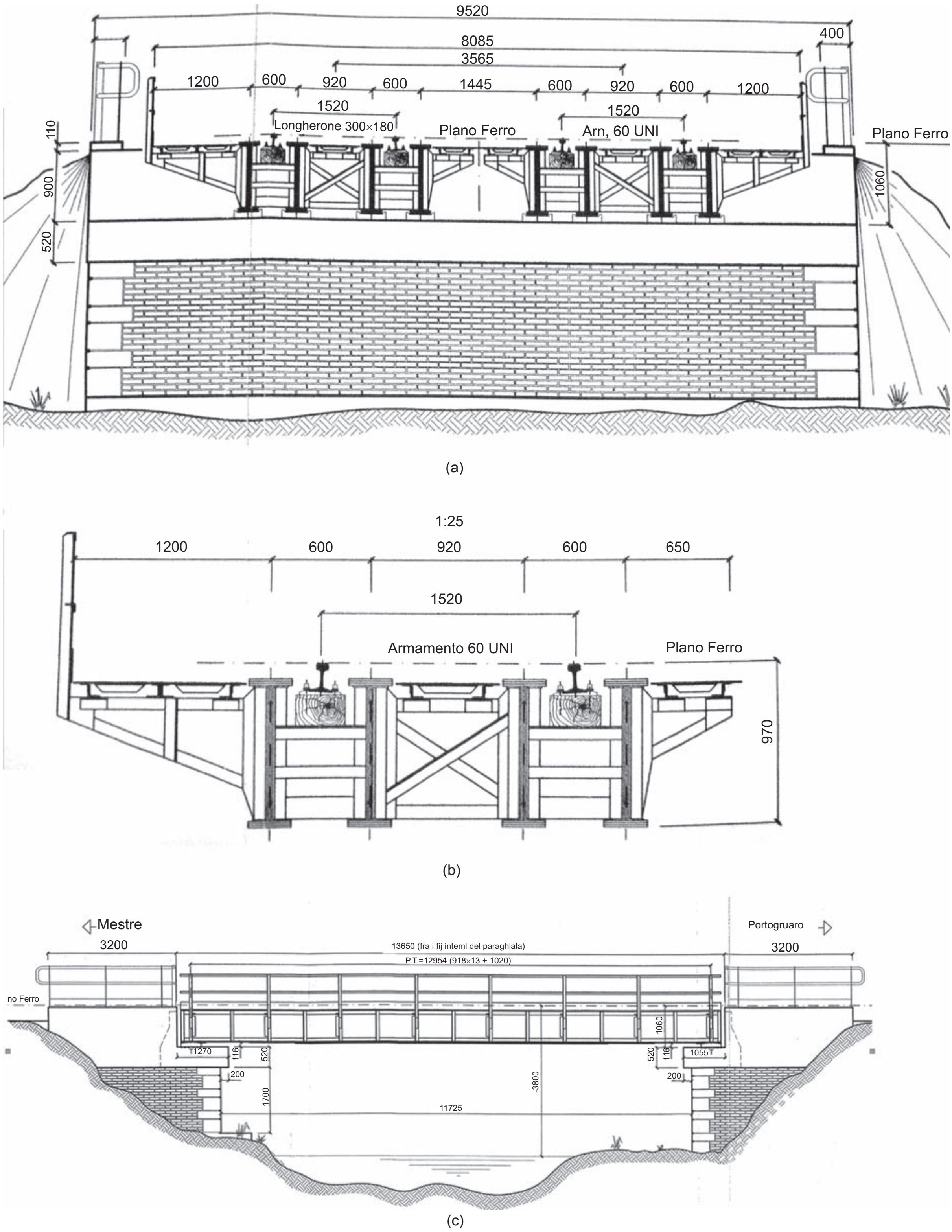

Figure 1. The Casaratta girder bridge (2009): (a) cross-section; (b) cross girder section; (c) lateral view (dimensions in mm)

service and most of them are at the end of their service life, which is attributed mostly to fatigue phenomenon. The current trend is to substitute short-span bridges, and to extend the life of medium span structures: for this reason, many minor riveted railway bridges have been dismantled, others are going to be replaced with new structures, while for larger structures interventions are needed in order to extend their lifetime. The average age of the 60% of Italian railway bridges which are steel is about one hundred years, as most were built between 1900 and 1920. Among historical metal bridges, riveted structures are the most common, and in this case some factors play an important role in the fatigue assessment as documented by several researches, such as Fischer *et al.* (1987), Mang and Bucak (1990), Matar and Greiner (2006), Boulent *et al.* (2008) and Albrecht and Lenwary (2009). Some studies concerning the research activity have been recently published, for example Pipinato *et al.* (2009a, 2009b) and are related to full-scale tests of old steel bridges, dismantled and assessed by testing, also taking into consideration material properties and their analysis. Two assessments of in-service bridges have also been published, investigating and assessing the remaining life of existing bridges (Pipinato and Modena, 2009; Pipinato *et al.*, 2010); moreover a comprehensive and innovative method to assess the reliability of existing bridges taking fatigue into account has been recently published (Pipinato, 2010). This paper particularly deals with the fatigue assessment of an old bridge structure, by adopting an analytical approach. The background motivation of the study derives from the fact that many bridges have been affected by fatigue failure (38·3% of the bridge collapses for JRC, 2008); also for this reason, many railway bridges have been dismantled even before reaching their expected service life (100 years). To enhance the confidence level on the fatigue performance of such bridges, both analytical and experimental assessments of the remaining life of dismantled bridges are required. In this paper the fatigue performance assessment of a case study bridge is carried out analytically taking advantage of the wide amount of studies developed in the past by the authors. This bridge has a very simple structural scheme widely used in the national network. Therefore the proper assessment of the remaining life, rehabilitation, reconstruction and repair is of wide interest. In this paper, the analytical fatigue assessment of this bridge is presented. The bridge is a riveted, multi-girder, steel structure, used for almost 95 years for train traffic. The fatigue assessment was carried out using the stress life approach as recommended by EC3-1-9 (BSI, 2005). Both static and direct integration dynamic analysis were carried out to estimate the stress time histories at critical hot spots. The stress ranges and the corresponding number of cycles were estimated using the rain flow method according to ASTM (2005). The fatigue strength of critical details was adopted from EC3-1-9 (BSI, 2005). The Miner's accumulated fatigue damage rule has been used to estimate the accumulated fatigue damage and the consequent remaining life. The approach takes its origin by integrating the parametric studies in a coded analysis to estimate the remaining life of the bridge: these parameters were uncertainties related to the train loads (traffic history and train speed) and to the fatigue strength code provisions for the bridge details.

2. Fatigue performance of riveted bridges

Railway bridges are subjected to cyclic repetitive axle loads over their entire life. These generate stress reversals which cause accumulation of fatigue damage and decrease in material strength capacity localised at specific structural details. Most of the bridge damage in the past has been attributed directly or indirectly to fatigue damage phenomenon: an estimate of 38·3% of the bridge collapses was reported by JRC (2008). In the following sections, typical fatigue damages are presented. Only details relevant for the case studies are illustrated.

(*a*) Damage to cover plates. In riveted girder steel bridges, the bottom flanges of the longitudinal girders are subjected to cyclic flexural tensile stresses. Fatigue cracks are usually initiated at discontinuities (e.g. the rivet holes).

(*b*) Crossbeam–longitudinal girder connection. The connection details between longitudinal and cross-beam of riveted railway bridges are subjected to cyclic shear plus to some extent flexure.

(*c*) Damage to riveted connections. Rivets used in longitudinal girders–cross beam connections are subjected to either single shear or double shear. If a structural detail is found unfit for fatigue performance, it can be retrofitted based on the stress cycle flow: hence different methodologies can be

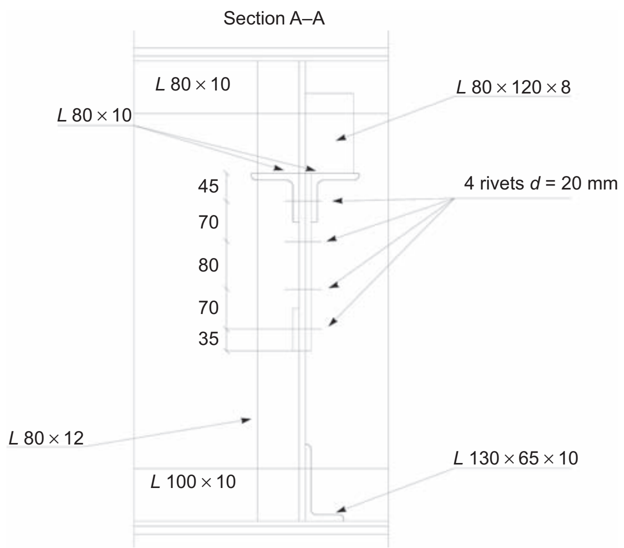

Figure 2. Geometric details of the cross-girder to longitudinal girder connection (dimensions in mm)

adopted for different details to take care of the fatigue stress-cycles.

For riveted girder steel bridges, the following retrofitting measures can be used:

(*a*) strengthening by means of high-strength friction grip bolts (HSFG) to replace the deteriorated rivets;
(*b*) additional structural members: the performance of the girder's flange can be enhanced by adding cover plates and webs can be enhanced by adding new angles;
(*c*) FRP interventions: the performance of flanges under cyclic flexural tensile stress can be strengthened by adding FRP straps;
(*d*) stop holes: fatigue crack propagation at discontinuities (stress concentration location) can be relaxed by providing stop holes;

Train type	Name	Train/day	Axle/day	Locomotive (L) and Carriages (Ci)	t/axle	Wagon number	Wagon type	Axle spacing: m
1	IC	20	960	L	20·25	1		2·6–6·4–2·6
	Intercity			C1	15	5		2·56–16·44–2·56
				C2	12·75	6		2·56–16·44–2·56
2	EC	10	340	L	20	1		2·85–2·35–2·85–2·35–2·85
	Eurocity			C1	14·25	2		2·56–16·44–2·56
				C2	12	5		2·56–16·44–2·56
3	EXPR	15	990	L	20	1		2·85–2·35–2·85–2·35–2·85
	Express			C1	14·25	10		2·56–16·44–2·56
				C2	12	5		2·56–16·44–2·56
4	DIR	30	1380	L	18·6	1		2·85–2·35–2·85–2·35–2·85
	Direct			C1	10·675	10		2·4–16·6–2.4
5	ETR	10	480	L	20	2		3–9–3
	Eurostar			C1	11·6	10		3–17·3–3
6	TEC	15	990	L	18·7	1		2·85–2·35–2·85–2·35–2·85
	Container freight			C1	20	15		1·8–12·8–1·8
7	Merci acciaio	10	720	L	18·7	2		2·85–2·35–2·85–2·35–2·85
	Steel freight			C1	20	15		1·8–13·06–1·8
8	Treno merci tipo D4	5	380	L	20	2		2·85–2·35–2·85–2·35–2·85
	D4 freight			C1	22·5	16		1·8–4·65–1·8
9	Treno merci misto	5	270	L	18·7	1		2·85–2·35–2·85–2·35–2·85
	Mixed freight			C1	16	24		9

Table 1. Instruction 44f (1992): daily traffic spectrum and train loads for fatigue verification

(*e*) repair of the bearing conditions: the corroded bearings can be replaced by new ones.

3. The case study

Concerning the service life history of the bridge, the case study is an old riveted railway bridge, built in 1918 and dismantled in 2005. A full geometric survey has been performed. The bridge has a twinned double girder, where the two main composite girders are connected with several cross-diaphragms. The bridge is simply supported on two abutments spanning 13·6 m. The cross-beams distance is 0·92 m, and wooden longitudinal beams lay on the cross-beams and distribute the load from the rail to the diaphragm of the girders. From on-site measurements and the existing drawings, the relevant geometric dimensions of the bridge required for structural modelling are reproduced in Figure 1, whereas Figure 2 shows the geometric details of the components used at the connection between the cross beam and the longitudinal girder. Once the geometry of the bridge was known, the traffic history was elaborated. This is a crucial step in fatigue calculation, because of the logarithmic dependence of stress to cycles. The Italian Railways Instruction 44/f (Italian Railway Authority, 1992). with trains passing through the bridge was adopted (Table 1), with nine different trains. Although it is clear that it cannot be assumed that the same traffic frequency occurred in the 1990s as well as in the year of construction, the same train type has been assumed, but with a traffic decrement in the range of 0 to 20% for every decade up to year 1918, as shown in Figure 3. This estimation is a simplified traffic model according to CER (2009).

4. Finite-element modelling and structural analysis

Because of symmetry, only one of the coupled girders is modelled: hence the cross braces are not explicitly modelled. The wooden longitudinal beams, which transfer the rail load to the cross girder, are modelled using lanes tool according to SAP 2000 (CSI, 2010). The axle loads are applied at five points of the sleepers in between the cross girders and distributed to three discrete points across the cross-girder. To evaluate the shear force distribution among the rivets, a refined finite-element model of a typical joint is generated using Ansys (2010). As the aim is to find the stress distribution among the rivets connecting the cross-girder to the longitudinal girder, the web of this is not included in the model. The angle connecting the cross-girder to the longitudinal girder, the rivets, the angles and the web plates of the cross-girder are explicitly modelled, as shown in Figure 4. Each component is independently meshed using solid elements, and the contact between each part is explicitly modelled using interface elements. The size of the meshes, both the contact and the solid elements, are iteratively refined until a more realistic converged stress distribution is obtained (Pipinato, 2008).

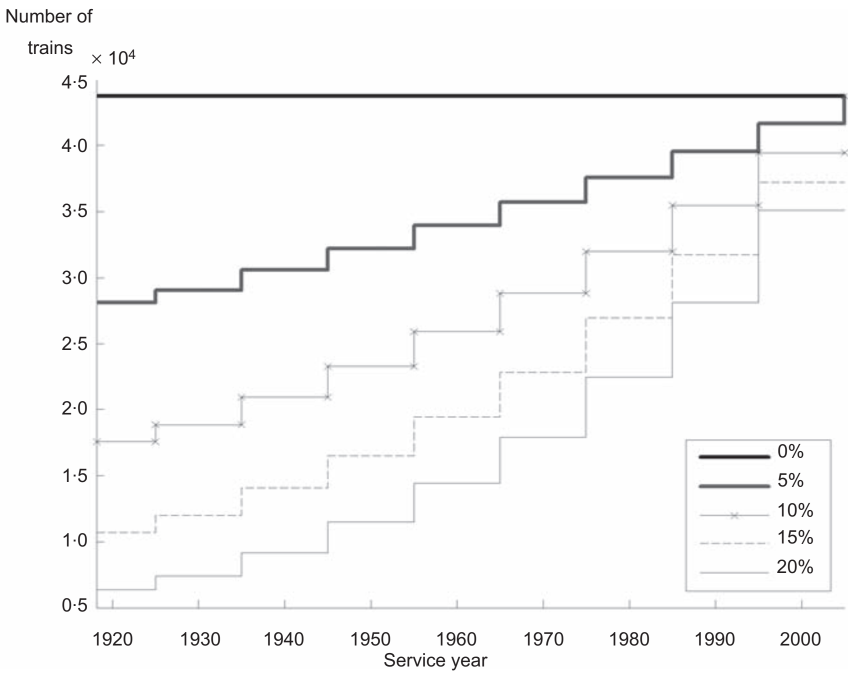

Figure 3. Possible ranges of train traffic trends across the Casaratta Railway Bridge

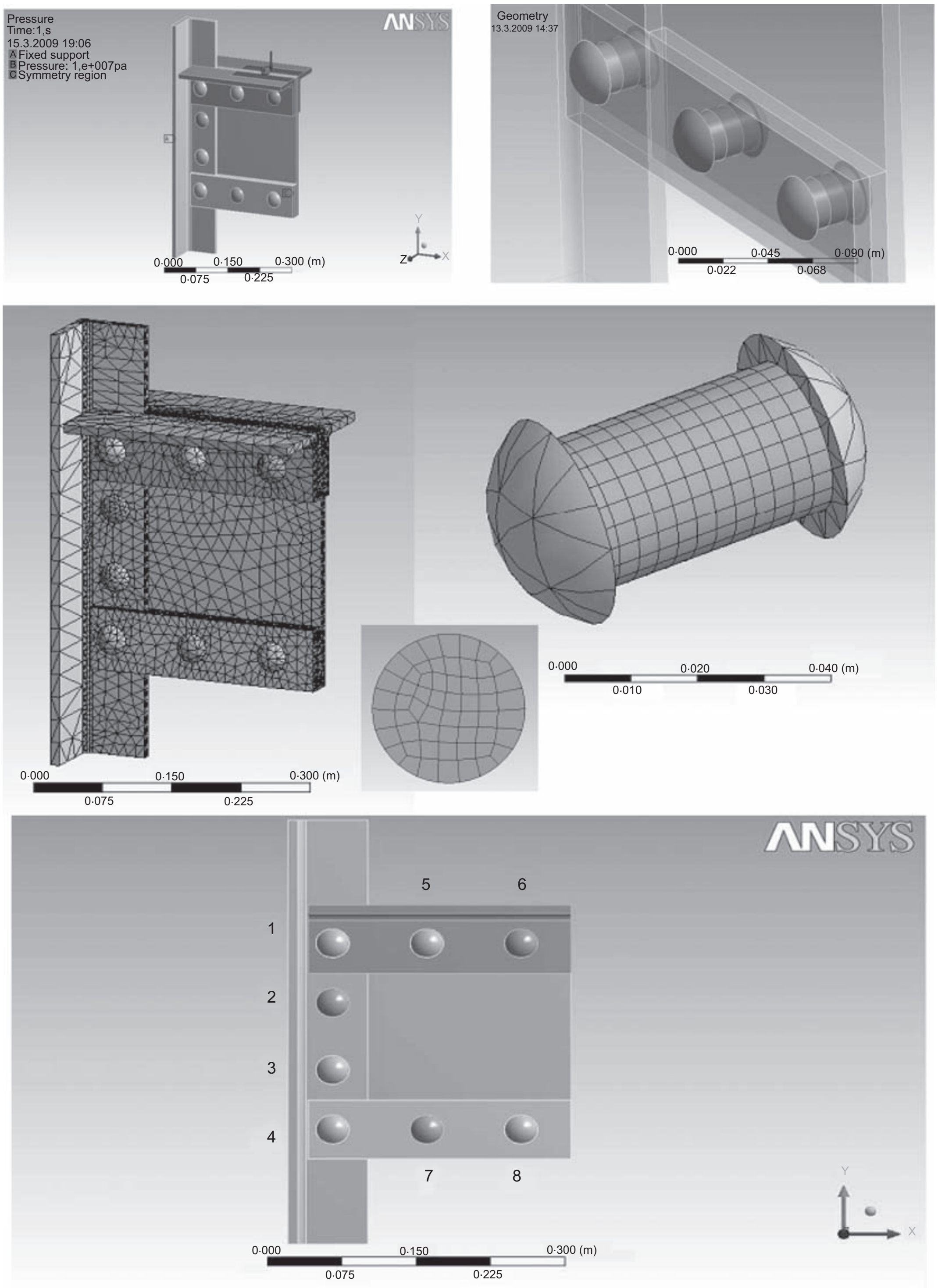

Figure 4. Geometric model of the joint

	I-Mode	II-Mode	III-Mode
Approximate	11·28		
Modal (SAP2000, CSI, 2010)	9·162	32·83	66·14

Table 2. Natural frequencies of the Casaratta Bridge

Figure 4 shows the finite-element meshes of different parts. Fatigue assessment of structural details using the S-N approach needs evaluation of stress ranges and cycles from stress histories obtained through either analytical simulation or monitoring during life. For determining the stress histories, EC1-2 (BSI, 2003) specifies either a simplified static approach or refined dynamic analysis based on the modal characteristics of the bridge and the speed of the trains. Hence, as a first step, the modal characteristic mode shapes, natural frequencies and modal damping of the bridge are studied. The modes of the bridge are identified by Eigen-value analysis (SAP2000, CSI, 2010). The modes' identification enables specification of the range of significant modes that has to be captured in the dynamic analysis. The specification of the damping matrix depends on the range of modal frequencies to be included in the analysis. The fundamental natural frequencies of the bridge were determined by the approximate formula given by EC1-2 (BSI, 2003) and by Eigen-value analysis using SAP2000 (CSI, 2010), and these values are given in Table 2. The approximate natural frequency, n_o [Hz], is given by

1. $$n_o = \frac{17{\cdot}78}{\sqrt{\delta_0}}$$

where δ_0 (mm) is the maximum mid-span deflection of the longitudinal girder under permanent loading. The modal damping should account for both the structural energy loss and the reduction of the axle loads owing to the inertial interaction between the bridge and the train. Given the span of the bridge structure (l), these damping values are given as follows

2. $$\xi[\%] = 0{\cdot}5 + 0{\cdot}125(20 - l)$$

Additional damping for inertial interaction

3. $$\Delta\xi[\%] = \frac{0{\cdot}01871 - 0{\cdot}00064l^2}{1 - 0{\cdot}0441l - 0{\cdot}004l^2 + 0{\cdot}00255l^3}$$

Total damping ratio

4. $$\xi_{tot} = \xi + \Delta\xi = 1{\cdot}9\%$$

The calculated modal damping is used for constructing the damping matrix for dynamic analysis. The dynamic response of the bridge under train loads depends on: the irregularities of the wheel–rail interfaces, accounted for by the dynamic amplification factor, φ''; train–bridge inertial interaction, accounted by additional modal damping, $\Delta\zeta[\%]$; and the correlation between the bridge's natural frequency with that of the trains' resonating frequency. To estimate the response of the bridge under train loads, two options are recommended by EC1-2 (BSI, 2003).

(*a*) The first approach is static analysis, in which the critical stresses are evaluated by applying axle loads statically and the response amplified by dynamic amplification factors provided by the code. This approach is allowed if the following conditions are satisfied: train speed < 200 km/h and natural frequency within the code bounds.
(*b*) The second approach is dynamic analysis: explicit dynamic analysis considering real trains is recommended if either of the above criteria is violated.

The frequency limit check is carried out and shown in Figure 5. As can be observed, the bridge satisfies the frequency requirement to use the static approach. However, the specified

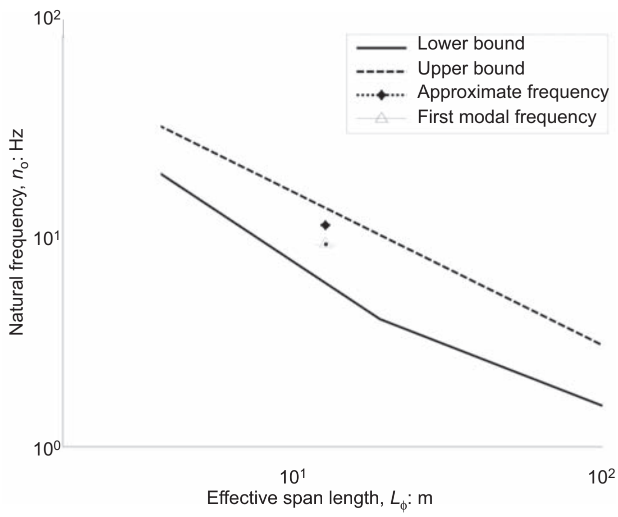

Figure 5. The fundamental frequency of the Casaratta Railway Bridge checked for the frequency bounds as specified in EN 1992

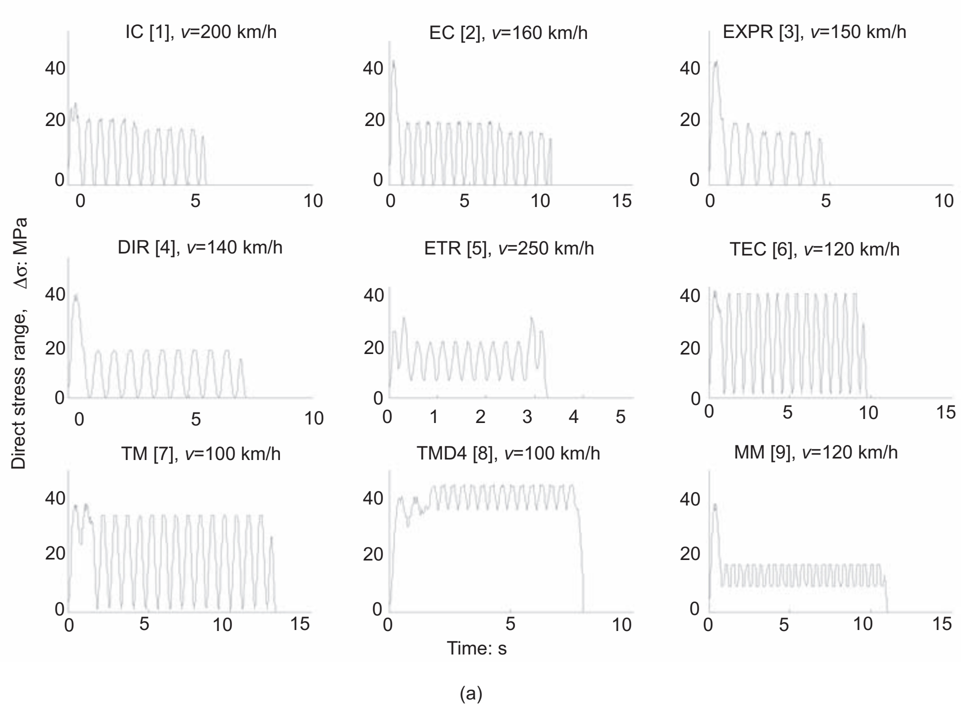

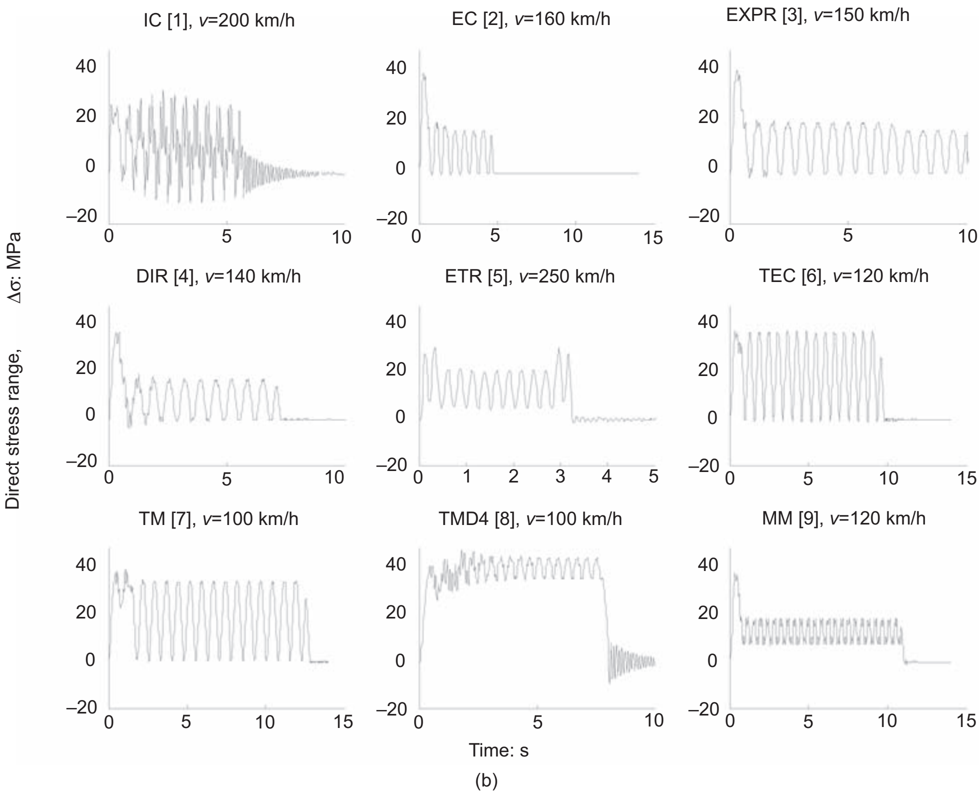

Figure 6. (a) Flexural stress time histories using multi-static analysis and (b) dynamic time history analysis

No.	τ_{max}: MPa	τ_{min}: MPa	% [max]	% [min]
1	13·27	−25·37	32	56
2	28·77	−31·28	69	69
3	32·62	−30·62	78	68
4	41·79	−45·04	100	100
5	7·94	−34·71	19	77
6	17·01	−28·89	41	64
7	4·92	−19·25	12	43
8	3·32	−7·88	8	17

Table 3. Shear stress distribution among rivets

commissioning speed of some train types exceeds the speed bound criterion. Hence both approaches have been carried out for the purpose of this project. In the multi-static analysis approach, the responses are evaluated by successive positioning of the axle loads on the discrete loading point lanes. The axle loads are repositioned every 0·02 s at the specified commissioning speed, and at each instant of loading the static equilibrium equation is solved. The sets of static equilibrium equations are given by

5. $$KU(t_t) = P_t$$

where

K is the global stiffness matrix of the bridge

$U(t_t)$ is the displacement vector of the bridge at discrete times

P_t is the set of axle load vectors at each discrete time.

In the dynamic analysis approach, the possible dynamic amplifications of the bridge response are directly determined, except those caused by impact effect owing to irregularities between the track and the train wheels: the train loads are represented as a series of spikes with duration equal to the time required to cross the bridge by each train. Each spike is represented as a triangular ramp load over discrete time intervals required to cross the adjacent discrete loading points. The dynamic equilibrium equation is given by

6. $$M\ddot{U}(t) + C\dot{U}(t) + KU(t) = P(t)$$

where

M is the global mass matrix of the bridge

K is the global stiffness matrix of the bridge

C is the global damping matrix of the bridge, built using Rayleigh proportional damping using the frequencies of the

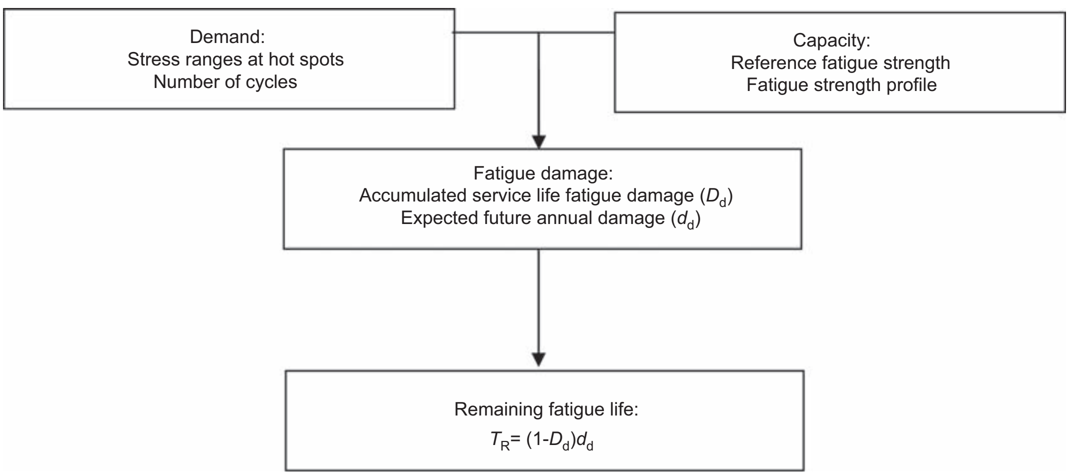

Figure 7. Fatigue assessment algorithm used for the Casaratta railway bridge

first and the fourth modes of the bridge with modal damping equal to 1·9%

$U(t)$ is the displacement time history vector of the bridge at discrete times

$\dot{U}(t)$ is the speed time history vector of the bridge at discrete times

$\ddot{U}(t)$ the displacement vector of the bridge at discrete times

$P(t)$ is the axle load time history vector of trains.

The responses obtained by this approach are amplified by the dynamic amplification factor to account for the effect of irregularities, which are not explicitly considered in the bridge model. The flexural tensile stresses at the extreme fibres of the bottom flange of the longitudinal girder are evaluated from flexural moments using spread sheets. The direct tensile stress time histories at the extreme bottom fibre of the longitudinal girder are amplified as

7. $$\Delta\sigma_{\mathrm{d}} = 0{\cdot}5(\varphi' + 0.5\varphi'')\frac{\Delta\sigma_{\mathrm{static}}}{\gamma_{\mathrm{Ff}}}$$
stress from multi–static analysis

8. $$\Delta\sigma_{\mathrm{d}} = 0{\cdot}5(0{\cdot}5\varphi'')\frac{\Delta\sigma_{\mathrm{Dynamic}}}{\gamma_{\mathrm{Ff}}}$$
stress from dynamic analysis (time history analysis)

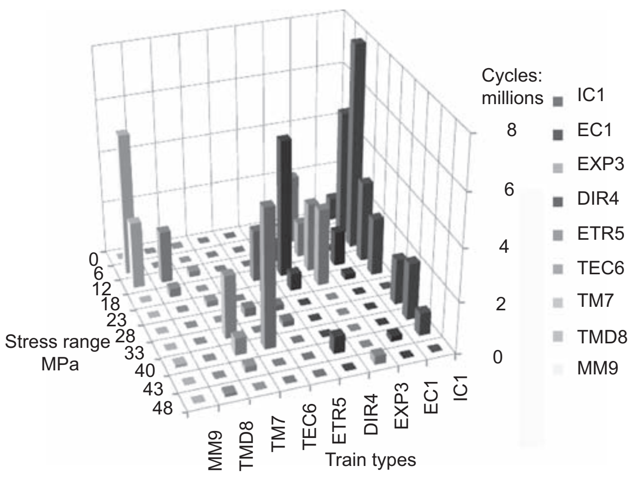

Figure 8. Flexural tensile stress range histogram for different types of train loading, evaluated from dynamic time history analysis at the specified commissioning speeds of trains

where

φ' is the dynamic amplification factor that accounts for the dynamic impact and is given by

$\varphi' = \dfrac{k}{1 - k + k^4}$ in which the parameter, k, is evaluated from

$$k\begin{cases} = \dfrac{v}{160}; \text{ for } L_\phi \leq 20 \text{ m} \\ \dfrac{v}{47{\cdot}16L^{0{\cdot}408}}; \text{ for } L_\phi > 20 \text{ m} \end{cases}$$

$\Delta\sigma_{\mathrm{d}} = 0{\cdot}5(\varphi' + 0{\cdot}5k\varphi'')\dfrac{\Delta\sigma_{\mathrm{static}}}{\gamma_{\mathrm{Ff}}}$ is the dynamic amplification factor that accounts for the effect of the irregularities of the

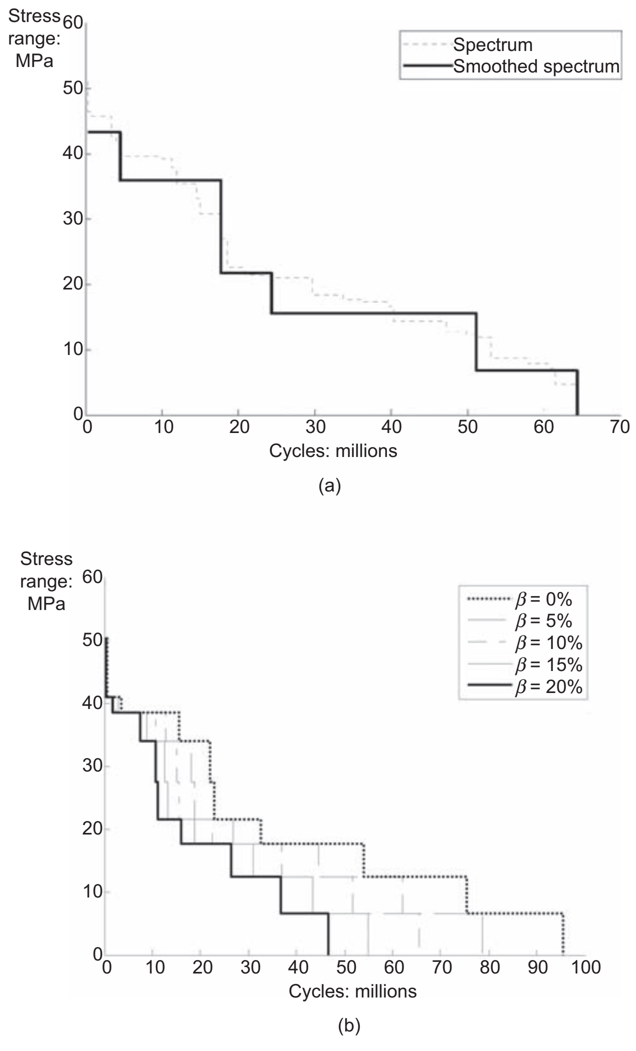

Figure 9. (a) Flexural tensile stress spectra, evaluated from dynamic time history analysis at the specified commissioning speeds of trains; (b) variation of flexural tensile stress spectra with traffic volume trend

interface between the rail and wheel and is given by

$$\varphi'' = 0{\cdot}56e^{\frac{L_\phi^2}{100}}$$

where v [m/s] is the commissioning speed of trains and L_ϕ [m] is the determinant length of the member.

The unfactored direct tensile stresses at the bottom flanges of the longitudinal girder are shown in Figure 6. As can be observed, the results of the multi-static and dynamic analysis are similar for all trains except for the first train type. The design shear stress in the rivets connecting the cross beam to the longitudinal girder is evaluated as

$$9. \quad \Delta\tau_\mathrm{d} = 0{\cdot}5(\varphi' + 0{\cdot}5\varphi'')\frac{\Delta\tau}{\gamma_\mathrm{Ff}}$$

where φ' and φ'' are described above. The unfactored shear stress in the rivets is evaluated by hand calculations assuming uniform stress distribution and by refined finite-element analysis (FEA) to account for the stress flow effect on stress distribution among the rivets, represented in Figure 4. Considering the axle load transfer mechanism from the cross-girders to the longitudinal girders by the rivets, the critical rivets are subjected to a shear stress of

$$10. \quad \Delta\tau = \frac{P}{18A_\mathrm{v}}; \quad P = \text{axle load}, \ A_\mathrm{v} = 0{\cdot}9A_\mathrm{g}$$

where A_g is the gross area of rivets and A_v is shear area of rivets. For circular cross-sections, the effective shear area is equal to 90% of the gross area. The analysis is carried out for the applied loads over an area where the wooden longitudinal beams are in contact with the cross-girder. As can be noticed

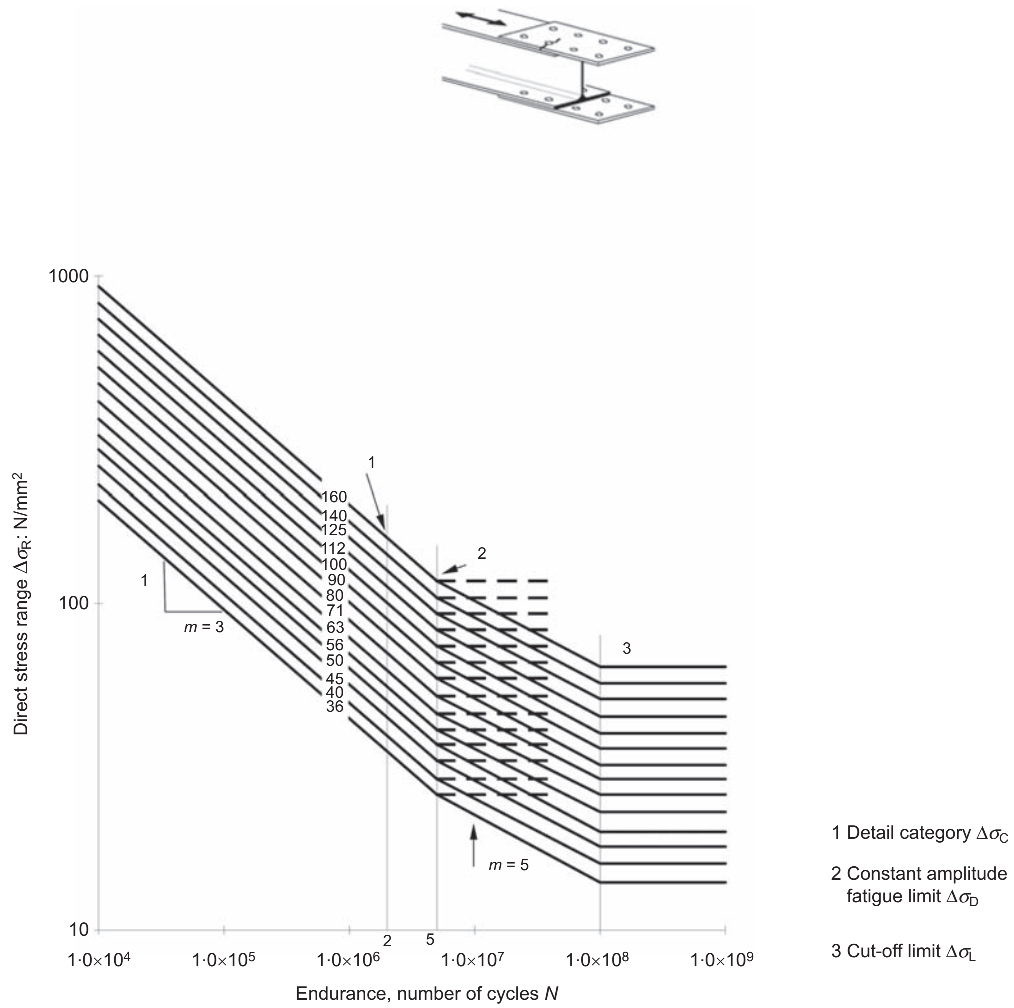

Figure 10. Fatigue strength curves for direct stress range

from Table 3, the bottom corner rivet is the critical hot-spot carrying the predominant shear; the shear stresses in the rivets owing to different axle loads, are obtained by scaling the axle loads in proportion to the shear distribution factors (Table 3).

5. Remaining fatigue life

The fatigue life of the case study is assessed according to EC3-1-9 (BSI, 2005), whereas the fatigue demand is evaluated from stress histories obtained in the previous sections. Miner's damage rule is used to calculate the accumulated fatigue damage indices and thereby to estimate the remaining fatigue life. The algorithm shown in Figure 7 is presented to illustrate this assessment. In order to estimate the remaining fatigue life of the structural detail, the fatigue demand should be presented as stress ranges plotted against number of cycles. Therefore, to cover demand spectra of the structural details owing to train loads, first the stress histogram is generated for each train by cycle counting and these histograms are then superimposed to find the total design spectra demand. The stress ranges and the corresponding cycles for each event of train passing are evaluated using the reservoir cycle counting method, according to ASTM (2005) and EC3-1-9 (BSI, 2005). These cycles for each stress ranges are then multiplied by the number of crossings during the service life of the bridge for each train. Figure 8 shows the stress histogram of the tensile detail for the considered traffic volume: histograms are generated from flexural tensile stress histories calculated using dynamic analysis. The stress histograms are superimposed to obtain the design stress spectra as shown by dotted lines of Figure 9: this plot is almost continuous and hence it allows the evaluation of the endurance from the capacity curve for each stress range. The spectral curve is smoothed and averaged over a series of frequency bands. For instance, the spectrum shown in Figure 9 is subdivided into five bands. The traffic trend, the

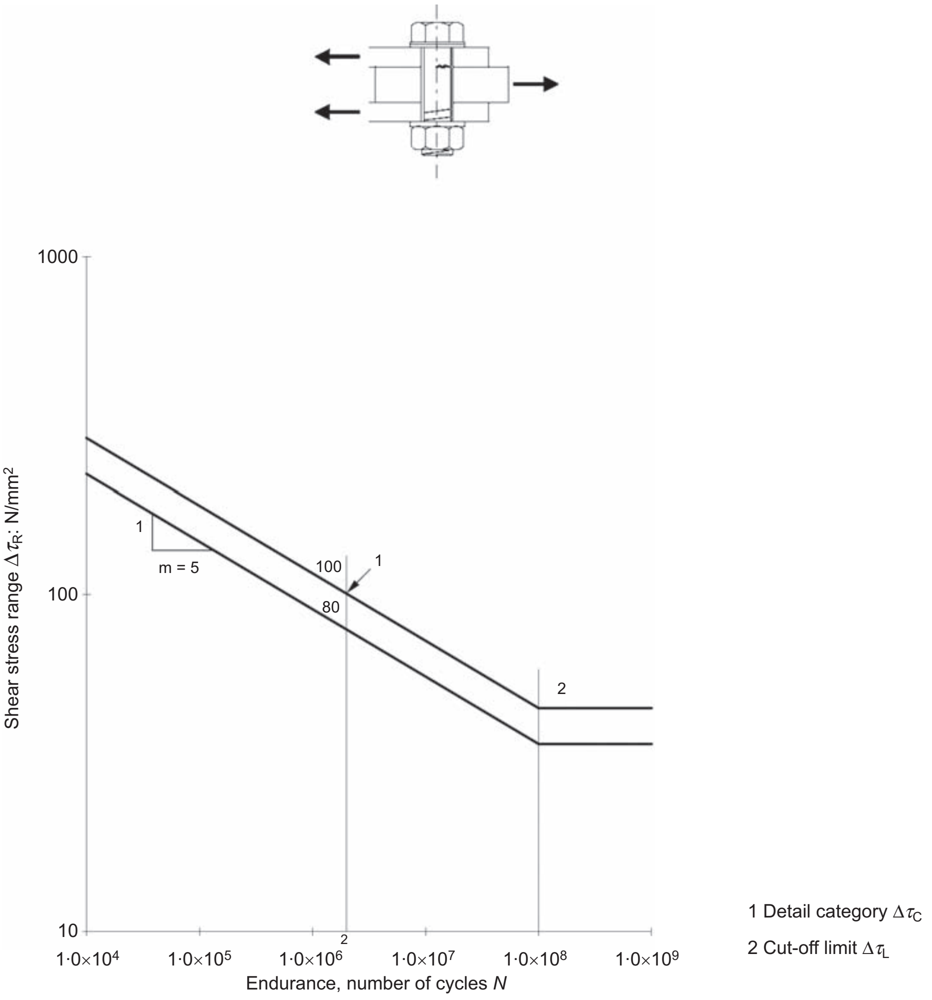

Figure 11. Fatigue strength curves for shear stress ranges

number of trains that crossed the bridge, is not known: Therefore to consider the possible bounds of the remaining fatigue life, the current traffic is decremented by fractions (β) ranging from 0% to 20%. This traffic volume variation affects directly the demand curve, especially the high-frequency stress ranges (Figure 10). In estimating the remaining fatigue life of an aged bridge, the most uncertain parameter is the fatigue strength of the structural details: the codes provide characteristic fatigue strengths. Strength profiles for predicting the strength for ranges of frequencies are also given. In order to account for the uncertainties of construction defects, maintenance level during service life and mode of failure, partial safety factors to reduce the specified characteristic strength according to the appropriate code are considered and reported in the analysis. The fatigue strength of the flanges of the girders under cyclic flexural tensile stress are estimated using EC3-1-9 (BSI, 2005) as reported in Figure 11. The specified characteristic strength depends on the degree of tightness between the bolt and the holes as well as on the preloading of the bolts. Therefore, three characteristic strengths (specified as detail category – DC) are provided: 50 MPa, 80 MPa and 90 MPa. As the real scenario in the rivets during service life of the bridge is unknown, all three possibilities are considered. Figure 11 shows the design strength for these cases: these curves are used for predicting the remaining fatigue of the detail in the following sections of this paper. As discussed above, the strength profiles and the characteristic strength of bolts under double shear is adopted for the rivets of this study, and again with reference to EC3-1-9 (BSI, 2005), a single characteristic value for bolts is given (C = 100). The fatigue curve used for this study is shown in Figure 12. Once the fatigue demand and strength for the critical structural details are specified, the next step is to evaluate the accumulated fatigue damage of the details according to the Miner's rule: for each stress range the number of cycles, n_t, and the endurance, N_t, are estimated from the demand and strength respectively. Then the ratio of imposed cycles to the endurance indicates the relative accumulated damage to the structural detail. Hence the total damage index, D_d, reported in Figure 12, is given by

11. $$D_d = \sum \frac{n_t}{N_t}$$

whereas the annual damage index, d_d, is given by

12. $$d_d = \sum \frac{n_t \text{year}}{N_t}$$

According to Miner's rule, the fatigue life of the structural detail is reached when the accumulated damage index is equal to one. Hence if a structural detail has experienced a D_d amount of damage during its service life and d_d amount annually, the remaining fatigue life of the detail, T_{RF} in years can be evaluated as

13. $$T_{RF} = \frac{1 - D_d}{d_d}$$

It is clear that the future traffic trend is unknown in advance; hence the equivalent annual damage indices are evaluated based on the current traffic volume. Parametric studies are carried out to observe the influence of uncertain parameters on

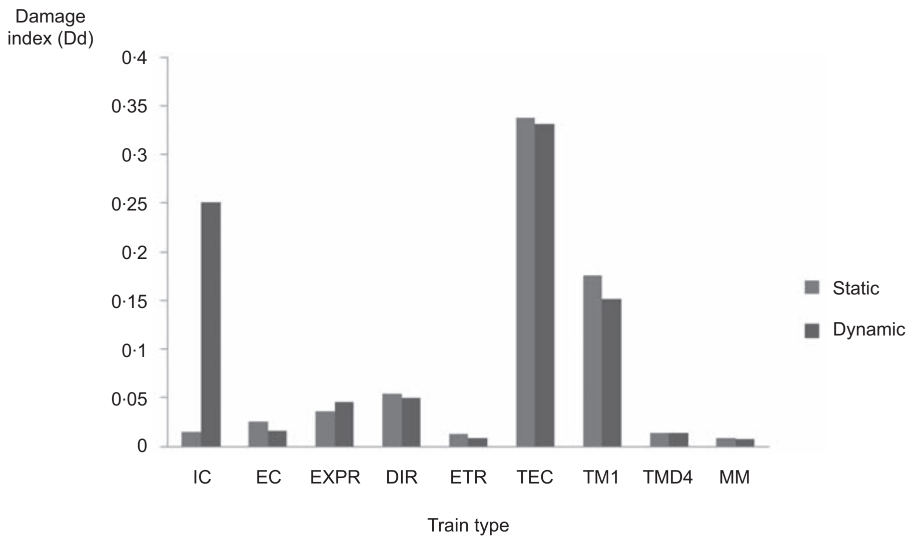

Figure 12. Accumulated damage indices of the tensile detail owing to different train loadings

the remaining fatigue life of the structural detail. The parameters are: traffic volume parameter β, describing the back traffic decrement of trains as a percentage for every 10 years; traffic speed parameter η, giving the ratio of the commissioning speed to the specified design speed of the trains; the design fatigue strength, accounted by the fatigue strength partial safety γ_{MF} and the characteristic fatigue strength of the detail, detail category [DC]. As described above, the traffic volume affects the demand spectra and hence the fatigue damage index. Figure 13 shows the contour plot of the remaining fatigue life of the flexural tensile detail of the longitudinal girder in years. The remaining fatigue life of the detail is consequently estimated. As can be observed, the design strengths below 80 MPa give negative fatigue lives, which means the detail would have failed before the service life of the bridge. This is unacceptable, as the bridge functioned properly until it was demolished; thus this detail category cannot be used for estimating the remaining fatigue of such riveted details. Similarly detail category 80 which is also on the boundary. Detail category 90 can be adopted for such details with appropriate partial safety factors. The adoption of detail category 90 can be further verified by experimental investigation of the demolished bridge. Considering the possibilities of the traffic decrement trend, the bridge could have been used for at least 15 additional years while complying with the failure criteria stated for the flexural detail. For this parametric study, the influence of the traffic speed on the demand spectra is accounted for by the dynamic amplification factors given by EC1-2 (BSI, 2003): direct dynamic analysis can be extended for this parametric study in the future. As shown in Figure 13 the remaining fatigue life (in years) of the structural detail reduces with the increase of commissioning speeds. The remaining fatigue life of shear details–rivets connecting the cross beam to the longitudinal girders is estimated following the same approach as that of the flexural tensile structural detail. The differences are represented by the fatigue strength (characteristic strength and curve profile) specification and the demand evaluation. Table 4 shows the ranges of the remaining fatigue life of the critical rivet. Considering the various possibilities analysed, it can be observed that the bridge has different remaining lives related with the different shear failure criteria.

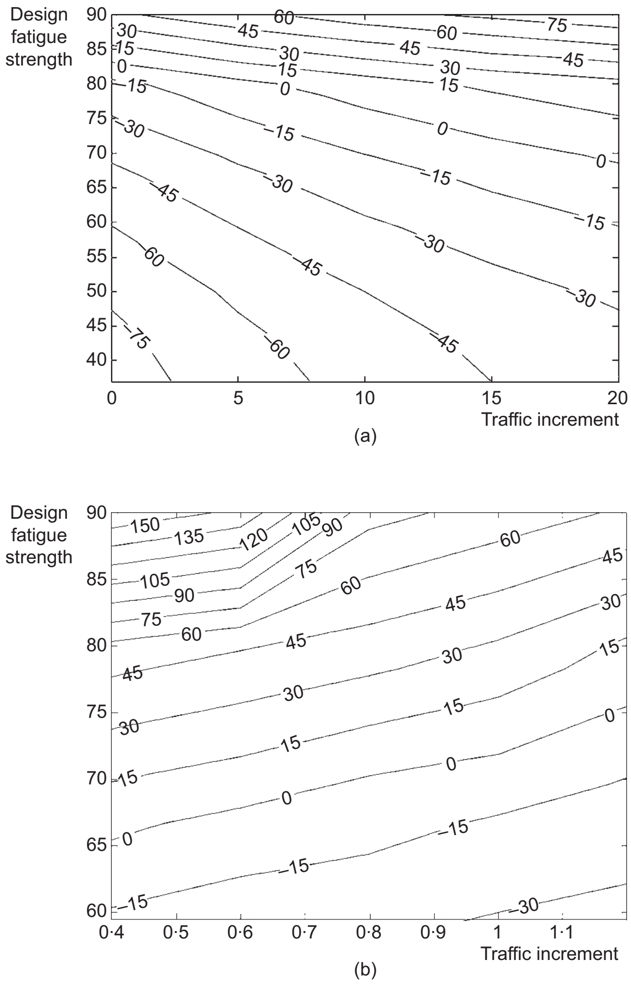

Figure 13. Ranges of predicted fatigue lives of the tensile detail resulting from uncertainties in traffic volume and fatigue strength specification depending on the traffic increment (a); same analysis considering the operating speed ratio

6. Conclusions

This paper deals with the fatigue assessment of historic metal riveted bridges. Previous studies have been critically reviewed to identify the parameters that affect the phenomenon. The review of damage scenarios associated with fatigue enabled identification of the critical structural hot spots, which are more susceptible for fatigue damage. In the case study the remaining life of a bridge is estimated analytically: the fatigue strength of the critical hot spots, the bottom flange of the longitudinal girder, which is subjected to high cycle flexural tensile strength, and rivets subjected to high cycle shear are estimated. The fatigue demand–stress ranges and number of cycles at the hot spots are estimated by carrying out both static and dynamic analysis using SAP 2000 (CSI, 2010) and Ansys (2010). The effect of train loads on the global structure has been simulated and the stress flow among the rivets estimated by a refined finite-element model of the girder joint using Ansys (2010). The remaining fatigue life of the critical details was estimated using spectral stress (S–N) approach as recommended by EC3-1-9 (2005). The Miner's accumulated damage rule is implemented to predict the fatigue damage indices. Based on the analytical fatigue assessment, conclusions can be drawn.

(*a*) The approximate dynamic amplification factors recommended by EC1-2 (BSI, 2003) significantly underestimates

		Detail category	
Dynamic amplification [φ]	Partial safety factor γ_{Mf}	DC100	DC71
0·5 (φ' + 0·5φ'')	1·00	8	1
	1·15	6	Damaged
	1·35	5	Damaged
0·25φ''	1·00	10	3
	1·15	7	1
	1·35	6	Damaged
1	1·00	14	5
	1·15	12	3
	1·35	9	2

Table 4. Remaining life of riveted connections

the fatigue damage induced by the train type IC on the riveted flanges of short-span railway steel bridges.

(*b*) For short cross diaphragms, the uniform shear distribution among rivets is not conservative.

(*c*) The fatigue life of a bridge is controlled by the rivets, at the connection of the cross-beams and the longitudinal girders, whereas the tensile flexural stress cycles acting on the bottom riveted flanges of the longitudinal girders is found to have a longer remaining fatigue life.

To enhance the confidence level in assessing the fatigue performance of riveted railway bridges, the following suggestions are proposed for further study

(*a*) a more rigorous study can be carried out to identify the effect of traffic speed on the demand spectra through dynamic analysis; parametric analysis investigating possible retrofitting methods

(*b*) experimental study to estimate the fatigue strength of the shear details of riveted connections.

Acknowledgements

The authors thank T. H. Birhane, J. Kocourek and E. Godde who implemented the analytical model in the research during their *Erasmus Mundus advanced masters in structural analysis of monuments and historical construction* in 2009, a master education programme co-founded by the EU-European Commission. Furthermore, all the analysis and conclusions reflects only the authors' view.

REFERENCES

Albrecht P and Lenwary A (2009) Variable-amplitude fatigue strength of structural steel bridge details: review and simplified model. *Journal of Bridge Engineering, ASCE* **14(4)**: 226–237.

Ansys (2010) *Complete Analysis Systems Guide*. Ansys Inc., Canonsburg, PA, USA.

ASTM (2005) ASTM E1049-85: Standard practices for cycle counting in fatigue analysis. ASTM, New York, USA.

Boulent MI, Righiniotis T and Chryssanthopoulos MK (2008) Probabilistic fatigue evaluation of riveted railway bridges. *Journal of Bridge Engineering, ASCE*, **13(3)**: 237–244.

BSI (2003) BS-EN-1991-2: Actions on structures. Part 2: Action on bridges. British Standards Institution.

BSI (2005) BS-EN-1993-1-9: Design of steel structures. Part 1.9: Fatigue. British Standards Institution.

CER (2009) International traffic data, Community of European railway and infrastructure companies, web site.

CSI (2010) *SAP2000 User Manual c.10*. CSI-Italia, Pordenone, Italy.

Fischer JW, Yen BT, Wang D and Mann JE (1987) *Fatigue and Fracture Evaluation for Rating Riveted Bridges*. Transportation Research Board, No. 302, Washington, D.C., USA.

Italian Railway Authority (1992) Instruction 44/f : Verifica a Fatica dei Ponti Ferroviari, Technical code of Italian Railway Authority (in Italian).

JRC (2008) JRC-2008: *Assessment of existing steel structures: Recommendation for estimation of remaining life.* JRC Scientific and Technical Reports.

Mang F and Bucak Ö (1990) Remaining fatigue life of old steel bridges – theoretical and experimental investigations on railway bridges. *Proceedings of International Symposium on Fatigue and Fracture in Steel and Concrete Structures*. 19–21 December 1991, Balkema Publishing, Madras, India.

Matar EB and Greiner R (2006) Fatigue test for a riveted steel railway bridge in Salzburg. *Structural Engineering International* **16(3)**: 252–260.

Pipinato A (2008) *High-cycle Fatigue Behavior of Historical Metal Riveted Railway Bridges*. PhD Thesis, University of Padova, Italy.

Pipinato A (2010) Step level procedure for remaining fatigue life evaluation of one railway bridge. *Baltic Journal of Road and Bridge Engineering* **5(1)**: 28–37, 2010, http://dx.doi.org/10.3846/bjrbe.2010.04.

Pipinato A and Modena C (2009) Structural analysis and fatigue reliability assessment of the Paderno bridge. *ASCE – Practice Periodical on Structural Design and Construction*, Posted ahead of print July 29, 2009 http://dx.doi.org/10.1061/(ASCE)SC.1943-5576.0000037.

Pipinato A, Pellegrino C, Bursi OS *et al.* (2009a) High-cycle fatigue behavior of riveted connections for railway metal bridges. *Journal of Constructional Steel Research* **65(12)**: 2167–2175, http://dx.doi.org/10.1016/j.jcsr.2009.06.019.

Pipinato A, Molinari M, Pellegrino C, Bursi O and Modena C (2009b) Fatigue tests on riveted steel elements taken from a railway bridge. *Structure and Infrastructure Engineering, Management, Life-Cycle Design and Performance*, Taylor & Francis, Abingdon, UK, http://dx.doi.org/15732470903099776.

Pipinato A, Pellegrino C and Modena C (2010) Assessment procedure and rehabilitation criteria for the riveted railway Adige bridge. *Structure and Infrastructure Engineering* http://dx.doi.org/15732479.2010.481674.

WHAT DO YOU THINK?

To discuss this paper, please email up to 500 words to the editor at journals@ice.org.uk. Your contribution will be forwarded to the author(s) for a reply and, if considered appropriate by the editorial panel, will be published as discussion in a future issue of the journal.

Proceedings journals rely entirely on contributions sent in by civil engineering professionals, academics and students. Papers should be 2000–5000 words long (briefing papers should be 1000–2000 words long), with adequate illustrations and references. You can submit your paper online via www.icevirtuallibrary.com/content/journals, where you will also find detailed author guidelines.